Towards Cardiac Angiographic Computed Tomography

Günter Lauritsch, Jan Boese, and Herbert Kemeth

***Abstract*– Minimal invasive, intra vascular, cardiac therapy would tremendously benefit from sophisticated image guidance. Currently tomographic imaging is available only offline by pre therapeutic CT scans. Recent developments in Angiographic Computed Tomography (ACT) allow 3D imaging of low contrast details with angiographic, C-arm based X-ray devices typically used during intervention. To take advantage of the improved contrast resolution a new approach for cardiac imaging is proposed which is based on intravenous contrast injection. The method is an analogue to the multi-segment reconstruction strategies in cardiac spiral CT. The challenge is to exclude movement in the reconstruction process as much as possible. Under the assumption of an almost periodic movement of the heart only those projection data are used for reconstruction which are acquired at a heart phase where the heart is expected to be almost in rest. Data gaps due to ECG-gating are filled by a series of *N* temporally complementary but spatially redundant scans. Temporal resolution is increased to *1/N* of the heart cycle time. Intravenous contrast injection allows for longer acquisition time to perform the series of scans. First results in simulation studies and in experimental phantom studies showed that excellent image quality could be achieved with the new method.**

I. Introduction

MINIMAL invasive, intravascular, cardiac therapy would tremendously benefit from sophisticated image guidance. Currently tomographic imaging is available only offline by pretherapeutical CT or MRI scans. It would be highly desirable to bring 3D imaging onto an angiographic, C-arm based X-ray device typically used during intervention. The main problem in cardiac tomographic imaging is the movement of the heart. In the literature several of approaches are reported based on an intra arterial injection of contrast agent. Movement is estimated from sets of projection images and compensated in the 3D reconstruction, see e.g. [1], [2]. However, these methods require numerous amount of user interaction which might not be appropriate for clinical routine.

Recent developments in Angiographic Computed Tomography (ACT) allow 3D imaging of low contrast details with angiographic X-ray devices in non-cardiac applications [3], [4]. To take advantage of the improved contrast resolution a new approach for cardiac 3D imaging is proposed which is based on intravenous contrast injection. The method is an analogue to the multi-segment reconstruction strategies in cardiac spiral CT [5], [6], [7]. The challenge is to exclude movement in the reconstruction process as much as possible. Only those projection data are used for reconstruction which are acquired at a heart phase where the heart is expected to be almost in rest. Minimal movement typically occurs in the end diastolic phase which can be detected in the ECG in a relative time window of typically 60-100% between subsequent R-peaks. Data gaps due to ECG-gating are filled by a series of temporally complementary but spatially redundant scans. Intravenous contrast injection allows for longer acquisition time to perform the series of scans

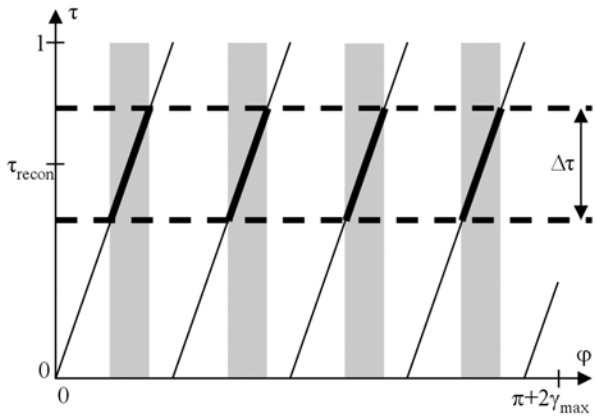

Figure 1: ECG-gated data acquisition. Only those projection data are used for image reconstruction which are acquired in a preselected window of the relative heart cycle time (gray shaded area).

II. ECG-Gated Image Reconstruction

In ACT a C-arm system typically covers an angular range of π + 2·fan-angle for circular short-scan reconstruction at a constant angular speed ω. Data acquisition is completed in typically 5-10 seconds depending on the number of projection images. The angular position of the X-ray source can be expressed as $\varphi = \omega \cdot t$ with time t. The cardiac phase τ ranges from 0 to 100% and indicates the phase within a current R-R-peak interval. Figure 1 shows, for an ideal acquisition, the correspondence of the angular position of the X-ray source φ to the cardiac phase τ. Projection data are selected in a time window centered at the reconstruction phase τ_{recon} with width $\Delta\tau$. The width $\Delta\tau$ determines the temporal resolution. At a heart rate of 60bpm typically 5-10 clusters of data are selected. Obviously there remain gaps in the selected data. The amount of missing data depends on the width $\Delta\tau$ of the time window.

Manuscript received November 2, 2005.

All authors are with Siemens AG, Medical Solutions, P.O. Box 1266, 91294 Forchheim, Germany (G. Lauritsch: telephone: +49-9191-18-9762, email: guenter.lauritsch@siemens.com; J. Boese: telephone: +49-9191-18-8992, email: jan.boese@siemens.com; H. Kemeth: telephone: +49-9191-18-8588, email: herbert.kemeth@siemens.com).

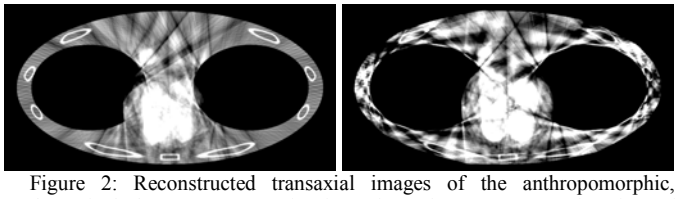

Figure 2: Reconstructed transaxial images of the anthropomorphic, mathematical phantom. ECG gating is performed at a reconstruction time of 90% of the R-R-peak interval. Top left: 1 run, no ECG gating. Top right: 1 run, ECG gating with τ_{recon}=90%, $\Delta\tau$=50%. Gray scale window C=0HU, W=400HU.

Thus, ECG-gated reconstruction runs in a trade-off between data completeness and temporal resolution. Figure 2 shows reconstructed images of a simulated heart phantom with and without ECG-gating. Obviously none of the both methods achieve tolerable image quality. Image degradations due to missing data are comparable or even more severe than those caused by movement.

III. Multiple Data Acquisition

The trade-off between data completeness and temporal resolution can be overcome by acquiring a series of almost identical short-scans. The phase or the start time of the scan is selected carefully such that each scan covers a complementary angular range in the desired time window. The total number N of scans required for data completeness depends on the temporal resolution to be achieved, and is given by $N \geq 1/\Delta\tau$.

A. Series of Forward Runs

Complementary data can be achieved by a series of N circular short-scan runs with the same angular speed. To make sure that subsequent runs are covering disjoint angular intervals in the required time window the starting time of the j-th run is triggered with a time delay $\tau_{0,j}^{f}$ relative to the R-peak of the ECG

$$\tau_{0,j}^{f} = (j-1)/N \quad \text{with } j = 1,...,N \,. \tag{1}$$

The time delay of the j-th run results in the coverage of an angular interval adjacent to the angular interval covered by the previous run (j-1). The covered angular intervals of all runs are equally distributed over the whole scan range. For a minimum number of runs $N_{\min} = 1/\Delta\tau$ the angular intervals are disjoint but seamlessly appended to each other. Data gaps would occur if the number of runs fell below the minimum number N_{min}. It is important to note that the time delay is independent of the required time window. Thus, with a series of forward runs, projection data can be selected corresponding to any reconstruction phase. In particular a dynamic sequence of image frames can be reconstructed from a single series of forward runs.

Acquiring a series of forward runs has a severe drawback. A significant amount of time is lost by driving the C-arm back to its start position without acquiring any projection data. In order to keep the overall acquisition time and the total amount of contrast agent administered to a minimum a more clinically viable solution consists of a series of alternating forward and backward runs.

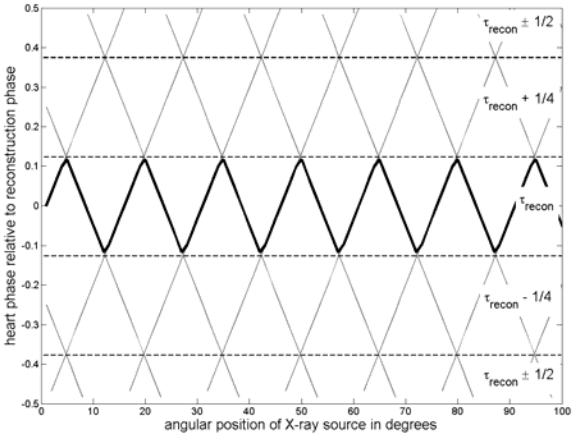

Figure 3: Heart phase versus angular position of the cone-beam source. An exemplary range of the scan is zoomed out. From four acquisition runs in altering forward and backward direction projections are selected (thick) which are confined within the time window of width $\Delta\tau$=1/4. The selected projection data form a zigzag curve. In total four zigzag curves can be created from that series of even numbered acquisition runs allowing to optimally reconstruct at four different heart phases.

B. Series of Alternating Forward and Backward Runs

The total time of data acquisition can be shortened significantly by acquiring projection images while the C-arm is returning to the start position of the next forward run. These runs in reverse direction will be called backward runs. For those runs acquired in the forward direction, Eqn. (1) still holds with a set of j indices restricted to odd numbers when beginning with a forward run. A proper time delay for the backward runs can be found by considering the fact that the angular positions φ of the X-ray source at the time instants associated with the reconstruction phase τ_{recon} should be the same as it would have been in a series of pure forward runs. Therefore for the backward runs the triggered time delay $\tau_{0,j}^{b}$ relative to the R-peak of the ECG can be expressed by

$$\tau_{0,j}^{b} = 1 - \tau_{end} + 2 \cdot \tau_{recon} - (j-1)/N \tag{2}$$

with j indices restricted to even numbers, and τ_{end} the heart phase at the end of the first forward run *(j=1)*. Equation (2) reveals that optimum triggering depends on the chosen reconstruction phase, and conversely, that a choice of triggering determines the optimum reconstruction phase. However, given a fixed delay time $\tau_{0,j}^{b}$ there is more than one optimal reconstruction phase τ_{recon}. Resolve Eqn. (2) to the form $2 \cdot \tau_{recon} = A$, where A is expressed in units of the cardiac phase and therefore is in the range from 0 to 1. There are two solutions for the optimal reconstruction phase, namely $\tau_{recon}^{(1)} = A/2$, and $\tau_{recon}^{(2)} = (A+1)/2$ due to the periodicity of the cardiac phase. In addition, as can be seen in Fig. 3 for an even number N of acquisition runs the temporal distribution of the

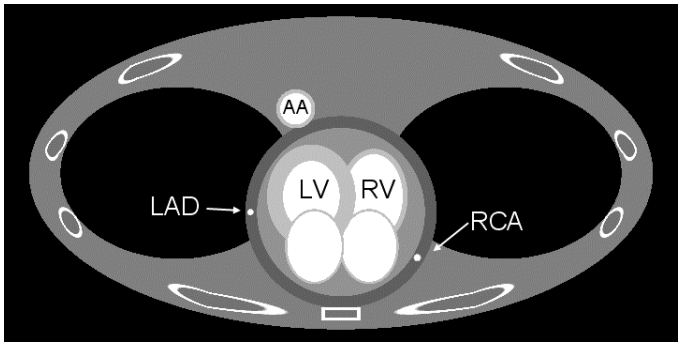

Figure 4: Sample transaxial slice of the mathematical heart phantom in the end diastolic phase τ=89.6%. Certain objects are indicated: right ventricle (RV), left ventricle (LV), aortic arch (AA), right coronary artery (RCA), left anterior descending artery (LAD).

angular position φ of the X-ray source shows a beneficial symmetry. Angular positions inside the time window of minimum extent are indicated by a black line which zigzags around τ_{recon}. Outside of that time window other zigzag curves can be found above and below. Thus, in addition to the selected reconstruction phase τ_{recon}, best temporal resolution is also achieved at $\tau = \tau_{recon} \pm i/N$ where i is any integer value such that $0 \le \tau < 1$. Unfortunately, in the case of an odd number N of acquisition runs, such simple symmetry does not exist. In conclusion, for reconstruction of a fully resolved 4D image stack, a series of pure forward runs are preferable. However, the clinical benefit of reducing the total acquisition time clearly outweighs the reduced flexibility in choosing the reconstruction phase retrospectively.

IV. Simulation Studies

A. Phantom Description and Parameters

Embedded in the FORBILD thorax phantom [8] a dynamic, mathematical model of a beating heart was designed [9]. Ventricles, atria, myocardium, epicardium, pericardium, aorta, aortic arch, and right and left coronary arteries are defined by a complex combination of ellipsoids and cylinders. A sample transaxial slice image is shown in Figure 4. The 3D movement of the heart is modeled by a set of intricate functions mimicking the anatomic motion according to clinical data found in the literature [10]. Right coronary arteries have a larger range of motion while left coronary arteries and myocardium show a significant rest period during the diastolic phase. The simulated motion field is quite challenging. The static, end diastolic phase is relatively short at less than 20% of the heart cycle time. In the sample transaxial image slice the maximum deflection of LAD and RCA is 1.8cm and 4.0cm, respectively. Maximum velocity of LCA and RCA during contraction and dilation is 15.4cm/sec and 25.0cm/sec. While this model may overestimate motion compared to clinical situations, our goal is to clearly work out the properties of the proposed method in a challenging scenario. A periodic motion of the heart is simulated with a constant heart rate of 75 beats per minute (bpm). The level of contrast agent is chosen to be

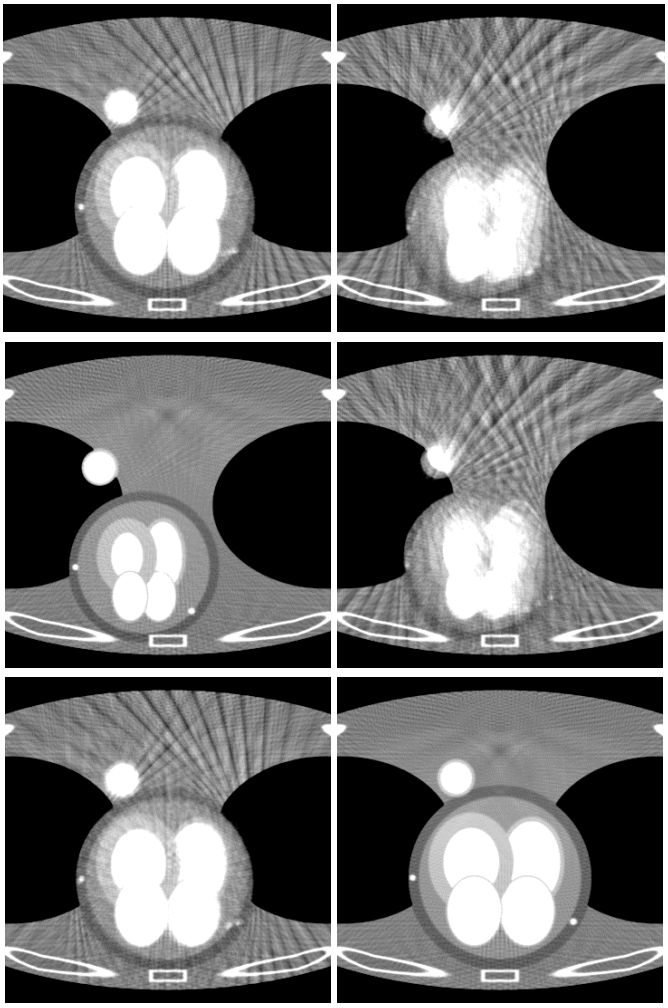

Figure 5: Dynamic sequence of transaxial images reconstructed from a single data set consisting of six acquisition runs in alternating forward and backward direction. The reconstruction phase τ_{recon} is 6.3% (top left), 22.9% (top right), 39.6% (middle left), 56.3% (middle right), 72.9% (bottom left), and 89.6% (bottom right) of the R-R peak interval. The cardiac phases 39.6% and 89.6% correspond to the systolic and the preferred diastolic phase, respectively. Gray scale window C=0HU, W=400HU.

300HU in the ventricles and aorta and 250HU in the coronary arteries.

The X-ray source and detector assembly is rotated along a circular arc of angular range 224° to cover π plus the full fan angle of the thorax phantom. 225 projection images are acquired each run at an angular increment of 1° per frame and 30 frames per second. Acquisition geometry is defined by a distance source to isocenter of 80cm and detector to isocenter of 40cm. The ideally absorbing planar detector consists of 1024×512 pixels of pixel side length 900μm in each direction yielding a detector size of 92cm×46cm. The parameters are chosen to avoid the problem of transaxial data truncation and to keep the amount of data reasonable. Projection data are computed free of noise with the SIEMENS in-house simulation software DRASIM (author Karl Stierstorfer).

Image reconstruction is performed with a conventional short-scan Feldkamp algorithm using Parker weights to deal with data redundancies. Temporal nearest neighbor interpola-

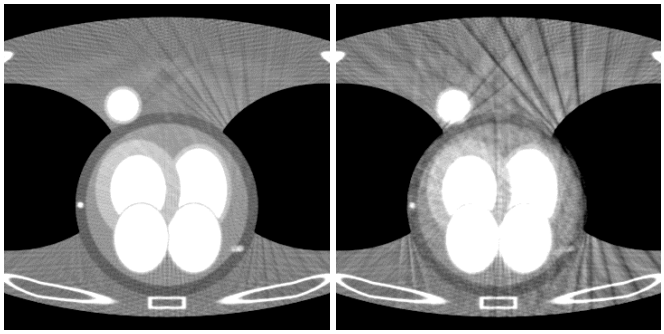

Figure 6: Variation of the number of acquisition runs. Transaxial image slice reconstructed from ECG-gated projection data of (left) N=3, and (right) N=2 acquisition runs in alternating forward and backward direction. Reconstruction phase τ_{recon}=89.6%. Gray scale window C=0HU, W=400HU.

tion is used in ECG gating. A 3D volume image with a voxel side length of 600μm in each direction is reconstructed, and a sample transaxial slice is selected and displayed.

B. Reconstruction of a Dynamic Image Sequence

From six acquisition runs, in addition to the triggered reconstruction phase τ_{recon}=89.6%, temporally optimal reconstruction is also possible at five other phase points τ=6.3%, 22.9%, 39.6%, 56.3%, and 72.9%. The phase τ=39.6% and τ=89.6% coincide with the systolic and diastolic phase, respectively, where almost no motion occurs.

Figure 5 shows the reconstructed image results. In the diastolic as well as in the systolic phase excellent image quality is achieved. Due to the small width of the ECG time window Δτ=1/6 even the right and left coronary arteries are clearly depicted. The images corresponding to phase instants τ=6.3% and τ=72.9%, which are both close to the static, diastolic phase still provide valuable information about the myocardium. The left coronary artery is somewhat blurred while the right coronary artery is totally degraded reflecting the fact that the duration of rest is much shorter for the RCA than for the LCA. Reasonable streak artifacts caused by data inconsistencies due to movement affect the image quality. At the phase points τ=22.9% and τ=56.3% strong motion occurs during contraction and dilation. The corresponding images are so degraded by blurring and strong streak artifacts that any valuable information is difficult to extract.

C. Number of Acquisition Runs

The optimal choice of the number of acquisition runs is a tradeoff between temporal resolution, dose, and total acquisition time. We therefore simulated data for six, three, and two alternating acquisition runs, which correspond to a width of the temporal ECG window of Δτ=1/6, 1/3, and 1/2, respectively. Figure 5, bottom right, and Figure 6 show image results at the reconstruction phase τ_{recon}=89.6%. In a reasonable time window centered at the chosen reconstruction phase the left coronary artery and the myocardium are in rest but the right coronary artery still shows some slight motion for some phases. The image resulting from three acquisition runs already shows some slight degradation relative to that from six runs. The right coronary artery appears a little blurred, and some slight streak artifacts are visible in the background. Certainly there is no rule for a tolerable image quality, as it will depend on the application and task. Due to cardiac motion, temporal resolution is almost equivalent to spatial resolution. For the depiction of large objects like the ventricles and the associated ostia of large blood vessels, temporal resolution may not be critical. For imaging of the small coronary arteries including some orders of sub branches, perfect temporal resolution is a prerequisite. These initial simulations also indicate that two runs will not satisfy clinical requirements in most cases.

V. Experimental Results

For a first validation of the simulation results some experiments are performed. A perspex resolution phantom is mounted on a slider and permanently moved parallel to the axis of rotation of the data acquisition system according to a sinusoidal law. The amplitude of the motion is 1.5cm at a frequency of 0.93Hz (equivalent to 56bpm) yielding a maximum speed of 1.4cm/sec. The phantom consists of a perspex panel of 1.1cm thickness with 12 rows of 5 boreholes each. The diameters of the boreholes are 0.40cm, 0.30cm, 0.20cm, 0.15cm, 0.12cm, 0.10cm, 0.09cm, 0.08cm, 0.07cm, 0.06cm, 0.05cm, and 0.04cm. Motion is perpendicular to the row direction.

To perform ECG-triggered multiple acquisition runs an experimental prototype controller software is installed on an AXIOM Artis *d*BA angiography system with a flat panel detector (Siemens Medical Solutions, Forchheim, Germany) A series of four runs in alternating forward and backward direction is acquired with 127 projection images at a rate of 30 frames per second and an angular increment of 1.5˚ each. The data of the 30×40cm^2 detector are rebinned to a pixel side length of 400μm in each direction. The distance isocenter to X-ray source is 75cm, isocenter to detector 45cm. Tube voltage is 70kVp, detector entrance dose 1.2μGray per frame. Projection data associated to specific phases of the motion are selected by an experimental prototype software offline and fed into a Feldkamp-type reconstruction software (DynaCT, Siemens Medical Solutions, Forchheim) using a smooth filter kernel. From the reconstructed 3D image volume multi planar reformatted (MPR) images are extracted with pixel side lengths of 400μm and 0.2cm slice thickness.

Reconstructed MPR images are displayed in Figure 7. In the static case the boreholes of diameter 700μm are clearly distinguishable. ECG-gating at a phase with minimal motion yields to an image result still resolving the boreholes of diameter 800μm. The slight loss of spatial resolution is due to residual motion in the selected projection data set. A slight blurring of the boreholes is observable. In the reconstructed image associated to the phase of maximal motion nothing can be resolved due to smearing and blurring. In the time window used for ECG-gating the positions of the boreholes are almost

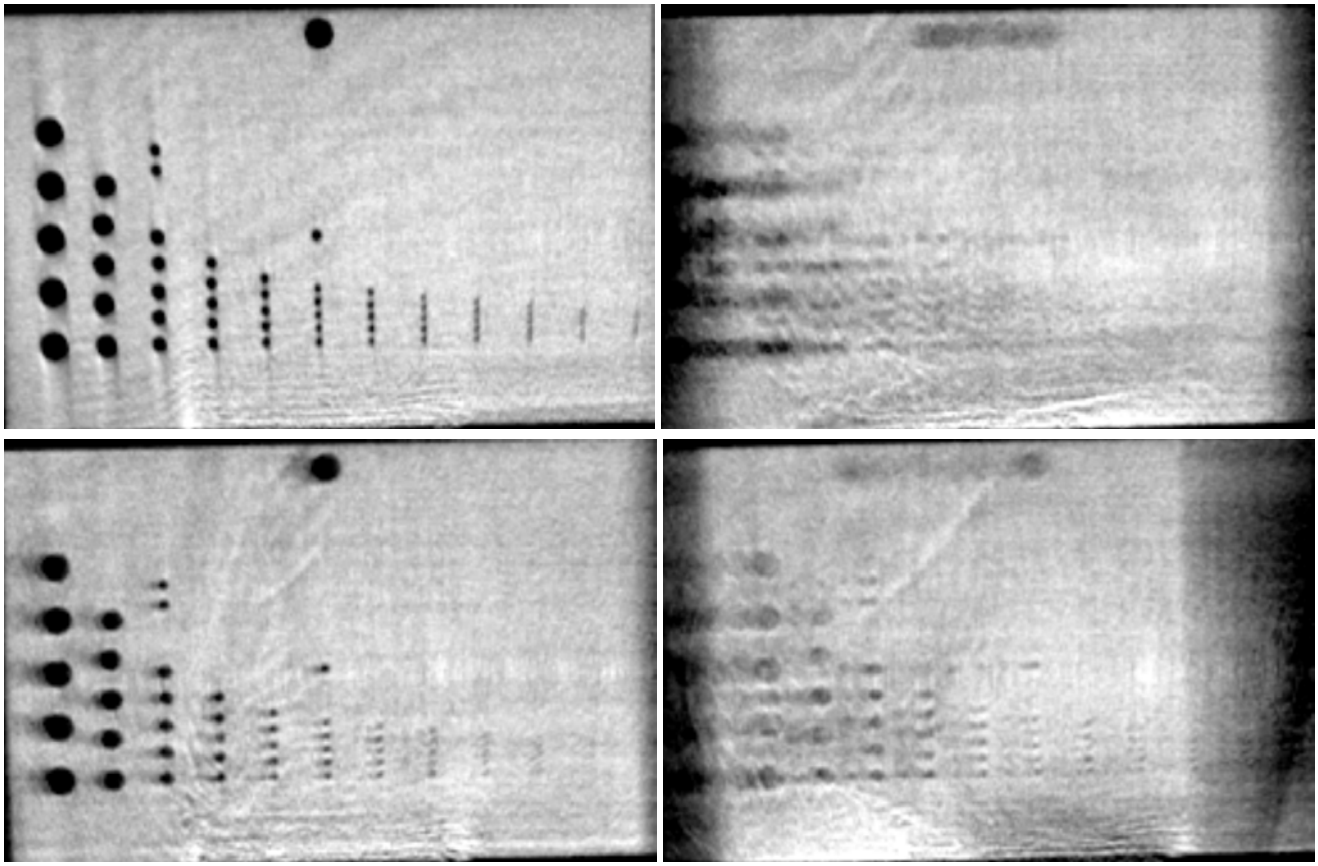

Figure 7: Reconstructed MPR images of a moving resolution phantom acquired with an experimental set-up. The MPR slice thickness is 0.2cm. Top left: static phantom. Top right: moving phantom reconstructed at the phase of minimal speed. Bottom left: moving phantom reconstructed at the phase of maximal speed. Bottom right: moving phantom reconstructed without ECG-gating. Gray scale window C=-150HU, W=700HU.

uniformly distributed in a range of 2.1cm. The benefit of ECG-gating can be most appreciated when comparing the image results with those without any ECG-gating. Without ECG-gating besides smearing a superposition of the two phases with minimal motion can be observed. No reliable information can be extracted from non ECG-gated images.

I. Conclusions

ACT with ECG-gated image reconstruction appears as a promising, viable way to provide real time, tomographic imaging for guidance of cardiac, intravascular interventions. Data completeness is assured by a series of temporally complementary but spatially redundant scans which can easily be acquired with little system modifications. ECG-gated image reconstruction only requires the additional step of temporal data selection. First results in simulation studies as well as in experimental phantom studies showed that an excellent image quality could be achieved. For clinical applications an ECG-triggered pulsing of the X-ray source might be used to significantly reduce patient dose.

Acknowledgment

We thank Rebecca Fahrig and Lars Wigström, Stanford School of Medicine, Department of Radiology, for their interest and the valuable discussions.

References

[1] C. Blondel, R. Vaillant, G. Malandain, and N. Ayache, "3D tomographic reconstruction of coronary arteries using a precomputed 4D motion field", *Phys. Med. Biol.*, vol. 49, pp. 2197-2208, 2004

[2] B. Movassaghi, V. Rasche, M. A. Viergever, and W. J. Niessen, „3D coronary reconstruction from calibrated motion-compensated 2D projections based on semi-automated feature point detection", *Proceedings of SPIE*, vol. 5370, pp. 1943-1950, 2004

[3] M. Zellerhoff, B. Scholz, E.-P. Rührnschopf, and T. Brunner, "Low contrast 3D-reconstruction from C-arm data", *Proc. SPIE,* vol. 5745, pp. 646-655, 2005

[4] G. Benndorf, C. M. Strother, B. Claus, R. Naeini, H. Morsi, R. Klucznik, and M. E. Mawad, "Angiographic CT in Cerebrovascular Stenting", *Am J Neuroradiol*, vol. 26, pp. 1813–1818, 2005

[5] T. Flohr, and B. Ohnesorge, „Heart-Rate Adaptive Optimization of Spatial and Temporal Resolution for ECG-Gated Multi-Slice Spiral CT of the Heart", *J. Comput. Assist. Tomogr.*, vol. 25, pp. 907-923, 2001

[6] M. Kachelriess, S. Ulzheimer, W. A. Kalender, "ECG-correlated imaging of the heart with subsecond multislice spiral CT", *IEEE Trans Med Imaging*, vol. 19, pp. 888-901, 2000

[7] T. Flohr, and T. Pan, "Image Reconstruction for ECG-Triggered and ECG-Gated Multislice CT", in *CT of the Heart*, U. J. Schoepf, Ed., Totowa, New Jersey: Humana Press, 2005, pp. 45-54

[8] http://www.imp.uni-erlangen.de/forbild/english/results

[9] A. Hölzel, "Dynamisches Herzmodell für die Computertomographie (CT) und Anwendungen für die CT-Herzbildgebung", master thesis, Fachhochschule Anhalt, Köthen, Germany, December 5, 2002

[10] S. Achenbach, D. Ropers, J. Holle, G. Muschiol, W. G. Daniel, and W. Moshage: "In-Plane Coronary Arterial Motion Velocity: Measurement with Electron-Beam CT", *Radiology*, vol. 216, pp. 457-463, 2000